Purdue University

Purdue e-Pubs

International Refrigeration and Air Conditioning Conference

School of Mechanical Engineering

2021

System Designing of Transcritical CO2 Air Conditioning Systems using Ejector Performance Maps

Muhammad Haider
University of Illinois at Urbana Champaign, United States of America, mhaider4@illinois.edu

Stefan Elbel

Follow this and additional works at: https://docs.lib.purdue.edu/iracc

System designing of transcritical CO₂ air conditioning system using the novel ejector performance maps

Muhammad HAIDER, Stefan ELBEL*

Department of Mechanical Science and Engineering,
University of Illinois at Urbana-Champaign,
1206 West Green Street, Urbana, IL, 61801, USA
Phone: (217) 244-1531, Fax: (217) 333-1942, Email: elbel@illinois.edu

* Corresponding Author

ABSTRACT

Awareness about the climate impact of air conditioning systems has given impetus in developing environment-friendly solutions. The transcritical CO₂ cycle with an ejector as a work recovery device has been reported as one of the green solutions in the literature. However, commercial applicability of these systems is limited so far despite their offered potential. One of the major impediments for limited commercial usage is unavailability of a systematic approach for system design that can help system designers in finding the optimum component combination for their application. For materializing system design approach, it is imperative to develop a system model that can accurately predict performance for wide range of operating conditions while considering different possible component combinations. In this paper, an ejector system model is developed using individual component models of ejector, evaporator, and compressor. The ejector is being modeled using the ejector performance maps, a recently developed methodology for representing ejector performance of a fixed-geometry ejector. The ejector performance maps are accurate, yet they can predict ejector performance for wide range of operation. The evaporator is modeled using geometric parameters, and the refrigerant and the air-side operating conditions, whereas other heat exchangers are modeled using thermodynamic state analysis. The compressor is modeled using semi-empirical correlations by curve-fitting ten-coefficient polynomial using compressor speed and pressure ratio as characterizing variables. The system analysis considers a total of eight component combinations for transcritical CO₂ ejector cycle and helps in finding the combination that gives the optimum performance. The results are encouraging as the system analysis using ejector performance maps can help in designing new improved systems. The methodology can also be tested for designing ejector air conditioning systems using other refrigerants.

1. INTRODUCTION

Current research in HVAC industry has been geared towards finding environment-friendly solutions. The CO₂ as a natural refrigerant offers a potential solution. However, due to its thermophysical properties, the CO₂ vapor compression cycle works as a transcritical cycle for a typical air conditioning application. This introduces significant throttling losses that accounts for lower system efficiency.

Ejector, working as work recovery device has been reported to improve system performance of a CO₂ transcritical system. Elbel and Hrnjak (2008) showed in one of the initial experimental studies that the system COP and cooling capacity of a transcritical CO₂ ejector refrigeration system can be simultaneously improved by up to 8% and 7% respectively. Nakagawa et al., (2011) showed experimentally that an internal heat exchanger can also improve the performance of a transcritical CO₂ ejector cycle by decreasing the quality at the evaporator inlet. Today, a transcritical CO₂ system can employ both an ejector and an IHX for improving the system performance.

The added complexity of a transcritical CO₂ system for improving its performance has not limited its usage in large systems like supermarket. However, this may be the reason hindering the penetration of CO₂ systems in other commercial applications like residential and automobile sector. One aspect of solving this added complexity is to develop robust design methodology that can help system design engineers in making system selection decision.

A system selection process typically involves component models based on experimental performance data from the manufacturers. The compressor performance maps are a typical example of such models. Recently, a similar model is proposed for a fixed-geometry ejector by developing ejector performance map from the experimental data (Haider and Elbel, 2020). These performance maps can predict the ejector performance using the ejector efficiency as the performance variable, whereas it only requires single operational variable of the volumetric entrainment ratio for characterizing the ejector performance. The performance map has been reported to predict the ejector performance accurately within 20% for wide range of operating conditions.

The ejector performance maps are computationally efficient, and yet accurate, which makes them practical to use in the system selection analysis. These performance maps are different from an evolving research area of physics-based ejector modeling. Aidoun et al., (2019) has summarized the latest developments in ejector physics-based models. The physics-based ejector models are computationally expensive, and their prediction may not remain accurate for wide range of operating conditions. The extended range for performance prediction is important as current research has shown that ejector can improve system performance through two mechanisms of power recovery and liquid recirculation (Pottker and Hrnjak, 2015). Most of the physics-based ejector models work with single-phase suction inlet conditions which tend to improve the system performance only through power recovery. However, the ejector performance map can accurately predict the ejector performance not only for single-phase suction inlet conditions, but also for two-phase suction inlet conditions. Thus, being computationally efficient and accurate for both single-phase and two-phase suction inlet conditions, the ejector performance maps have advantage over physics-based ejector models when conducting system selection analysis as system performance can be evaluated for larger operational envelope.

For developing a robust design methodology for a CO_2 transcritical system, it is imperative to develop a detailed system model that can predict the system performance from the experimental performance of individual components. Each component plays an important role in determining the system performance. For example, Lawrence and Elbel (2018) showed numerically that evaporator design can improve ejector refrigeration system performance. Also, the system performance can be improved by changing the IHX effectiveness (Nakagawa et al., 2011). There is no published work to the best knowledge of authors that highlight the effect of compressor performance on the ejector system performance.

The added complexity in a transcritical CO_2 ejector system makes the system modeling of such a system also a challenge. Typically, a vapor compression system is modeled using enthalpy marching scheme. In a typical vapor compression cycle, the system can be solved only by considering low-side and high-side pressure while propagating the enthalpy from the compressor inlet to the other components. The compressor inlet enthalpy can be known based on the evaporator desired exit conditions. However, presence of the internal heat exchanger involving parallel flow conditions within in the cycle along with split and merger of different streams in the separator and ejector respectively, makes junction solver scheme an appropriate choice (Winkler et al., 2008). The junction solver scheme considers pressure and enthalpy at each inlet and exit port of the component while system is solved for energy and mass balance. This, however, makes solver computationally expensive and the system model may not remain practical.

In this study, the enthalpy marching solver scheme is used, making the solver computationally less expensive than junction solver scheme. The enthalpy marching solver is computationally efficient because it uses less variables to solve the system than junction solver scheme. A transcritical CO_2 ejector system model is developed for predicting the system performance for different combinations of components. For the sake of brevity, the effects of only three components namely ejector, evaporator and compressor are considered. In the first part, the component and system models are introduced. In the second part, the validation of component models and system model is presented. In the last part, the system analysis is carried out while considering eight possible component combinations. The combination giving the maximum COP and capacity during the analysis is selected as the final system.

2. EJECTOR SYSTEM MODEL

A system model for a standard transcritical CO_2 ejector cycle with internal heat exchanger (IHX) has been developed in MATLAB for predicting system performance using different combinations of the system components. The fluid properties are obtained using CoolProp (Bell et al., 2014). The system schematics for the standard ejector cycle with an IHX is shown in Figure 1. A total of three variables P_{cpri}, P_{eri} and $\phi_m = \dot{m}_{sn}/\dot{m}_{mn}$ are used for finding the solution of the ejector system for a given high-side pressure. The constraint equations satisfy the evaporator exit condition, system energy balance, and the ejector pressure lift as the difference between evaporator exit and IHX

suction inlet pressure. It is assumed that the separator is non-ideal and some of the liquid droplets enter the suction line of the IHX. The internal heat exchanger and gas cooler are modeled using thermodynamic state analysis. The details of other component models are as follows:
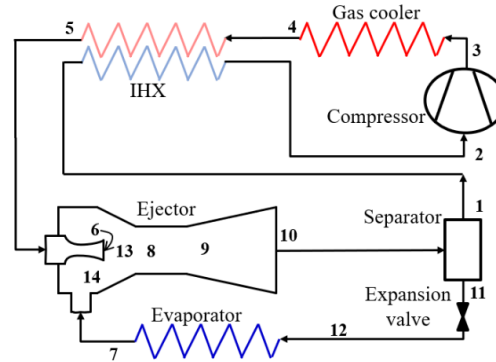
Figure 1: Schematics of standard ejector system with internal heat exchanger

2.1 Ejector modeling

The ejector is modeled using recently proposed ejector performance maps (Haider and Elbel, 2020). The performance maps use volumetric entrainment ratio, ϕ_v as the characterizing variable, and a new definition of ejector efficiency $\eta_{ejec,map}$ as performance variable. The ejector efficiency, $\eta_{ejec,map}$ is given by Equation (1)

$$\eta_{ejec,map} = \frac{\dot{m}_{mn}(h(P_{dro}, s_{mix}) - h_{mix}}{\dot{m}_{mn}(h_{mn,in} - h(P_{sn,in}, s_{mn,in})} \tag{1}$$

The volumetric entrainment ratio, ϕ_v is given by Equation (2)

$$\phi_v = \frac{\dot{v}_{sn}}{\dot{v}_{mn}} = \phi_m \frac{\rho_{mn}}{\rho_{sn}} \tag{2}$$

The performance map for a fixed-geometry ejector can be obtained by curve-fitting experimental data using second order polynomial given by Equation (3).

$$\hat{\eta}_{ejec,map} = C_1 + C_2\phi_v + C_3\phi_v^2 \tag{3}$$

In this study, two ejectors are considered. The data for Ejec A is from Haider and Elbel (2020), while the data for Ejec B is from Zhu et al., (2017). The performance maps for both the ejectors are shown in Figure 2.
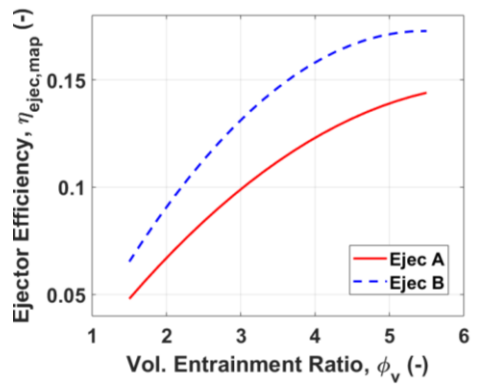
Figure 2: Ejector performance maps for the two ejectors used in the study

2.2 Evaporator modeling

The microchannel evaporator has been modeled by discretizing it into finite volumes. The flow inside the evaporator is counter-crossflow with dry conditions on the air side. The energy balance is solved inside each of the finite volumes while calculating refrigerant and air-side heat transfer coefficients using empirical correlations specified in Table 1. The pressure drop is only considered on the refrigerant side while fixed mass flow rate is assumed for the air side flow. The evaporator is solved iteratively by updating temperatures and pressures in each volume from previous

iteration, until the exit condition variations are below the set tolerance. The finite volume in which refrigerant flow changes from two-phase to single-phase condition, is further resolved in to two separate regions for calculating heat transfer and pressure drop using respective correlations. This allows using lower number of elements to discretize the evaporator. In this study, the evaporator is discretized into 10 elements per slab.

Table 1: Empirical correlations used for modeling evaporator

	Parameter	Reference
Pressure drop	single-phase refrigerant DP	Churchill (1977)
	two-phase refrigerant DP	Friedel (1979)
HTC	single-phase refrigerant HTC	Gnielinski (1976)
	two-phase refrigerant HTC	CO_2: Shah (2017)
	Air-side HTC	Park and Jacobi (2009)

For analysis, two microchannel evaporators are used in this study, both having four slabs and single pass. The dimensions for Evap A are given in Zhu et al., 2018. The Evap B differs with Evap A only in port diameter. Evap A has a port diameter of 0.81mm whereas, Evap B has a port diameter of 0.53mm. The experimental data is only available for Evap A, and it is assumed that the model will account for the change in performance of the evaporator if the port diameter is changed by the given amount.

2.3 Compressor modeling

The compressor performance is modeled using three efficiencies for predicting specific quantity related to compressor performance. The volumetric efficiency, η_{vol} relates the mass flow rate with the compressor suction inlet conditions, and compressor operating conditions. Thus, $\hat{\eta}_{vol}$ helps in predicting mass flow rate for the given compressor operating conditions. The volumetric efficiency, η_{vol} can be measured by experimental data using Equation (4).

$$\eta_{vol} = \frac{\dot{m}_{meas}}{\rho_{suc}CN} \tag{4}$$

The compression efficiency, η_{comp} gives the ratio between ideal and actual work required for the compression. The $\hat{\eta}_{comp}$ helps in predicting the discharge temperature. It can be measured using Equation (5)

$$\eta_{comp} = \frac{\dot{W}_{isen}}{\dot{W}_{act}} \tag{5}$$

The compressor power is also an important performance variable which can be predicted using the isentropic or overall efficiency $\hat{\eta}_{isen}$. The measured isentropic efficiency η_{isen} is given by Equation (6)

$$\eta_{isen} = \frac{\dot{W}_{isen}}{\dot{W}_{elec}} \tag{6}$$

The measured efficiencies from selected experimental data points for different compressor speeds and pressure ratios are used to curve-fit 10-coefficient polynomials for each of the efficiency using the pressure ratio, $\beta = \frac{P_{dis}}{P_{suc}}$ and the normalized compressor speed, $N_{norm} = \frac{N}{N_{rated}}$ as the two characterizing variables. The 10-coefficient polynomial for each efficiency can be written in the general form using Equation (7)

$$\hat{X} = C_1 + C_2.\beta + C_3.N_{norm} + C_4.\beta^2 + C_5.\beta.N_{norm} + C_6.N_{norm}^2 + C_7.\beta^3 + C_8.N_{norm}.\beta^2 + C_9\beta.N_{norm}^2 + C_{10}N_{norm}^3 \tag{7}$$

where $\hat{X}$ can either be $\hat{\eta}_{vol}$, or $\hat{\eta}_{comp}$ or $\hat{\eta}_{isen}$. In this study, two compressors are used for analysis. However, the experimental data has been collected using the same compressor available in the lab facility. The compressor is a CO_2 semi-hermetic radial piston-type variable speed compressor. The performance map of two different compressors is obtained by collecting experimental data at two different cooling conditions for compressor. The Comp A represents data collected while the compressor is cooled using a fan, whereas Comp B represents data collected when the compressor is cooled through natural convection. The power consumed by fan for Comp A is not included in any calculations. The difference in the cooling mechanism is used in making a single physical compressor, work as two different compressors (Haider and Elbel, 2020).

3. MODEL VALIDATION

This section presents the validation results for predicting the performance of individual components, as well as for predicting the system performance. The experimental data for model validation is obtained by the lab facility shown in Zhu et al., 2018.

3.1 Components validation

The prediction accuracy for each component is important in determining the overall system prediction accuracy. The performance map can predict ejector performance within 20% of accuracy using the data for Ejec A (Haider and Elbel, 2020). The performance map uses only the single-phase suction inlet data points for curve-fitting the second order polynomial, while it can also predict accurately the ejector prediction for two-phase suction inlet conditions. The compressor power and the mass flow rate for Comp A and Comp B can be estimated within 5% accuracy (Haider and Elbel, 2020).

The validation result for the evaporator model is shown in Figure 3. The model can predict within 10% of capacity for both single-phase and two-phase evaporator exit conditions.
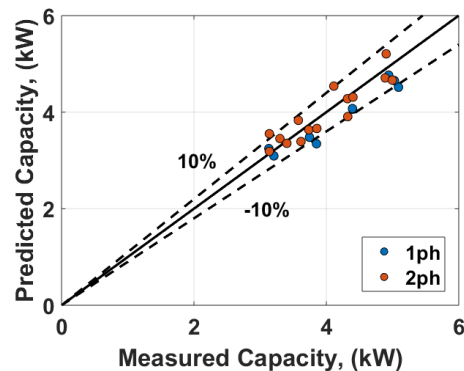
Figure 3: Predicted vs measured capacity of Evap A

3.2 System validation

The data for validating system model is collected for wide range of operating conditions. The data points have both single and two-phase evaporator exit conditions. The ambient temperature is in the range of 35-45°C, while compressor speed is in the range of 900-1500min^{-1}. The suction inlet quality for IHX is taken from experimental data as one of the parameters for each of the simulation point. Figure 4 shows the solver can predict system COP within 10% for most of the data points.
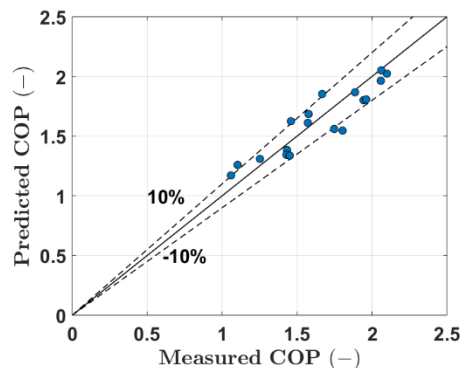
Figure 4: Prediction of system COP

4. ANALYSIS AND DISCUSSION

The study considers two ejectors, two evaporators, and two compressors for system analysis. Thus, a total of eight combinations are possible that have been labelled as shown in Table 2 for ease in reporting results.

Table 2: Eight component combinations considered in the study

Comb	Comp	Ejec	Evap
1	A	A	A
2	A	A	B
3	A	B	A
4	A	B	B
5	B	A	A
6	B	A	B
7	B	B	A
8	B	B	B

Some of the key simulation parameters are listed in Table 3. These parameters are not changed during any of the simulation. No pressure drop is assumed in the suction line of IHX.

Table 3: Key simulation parameters

Parameter	Value	Unit
Evaporator air inlet temperature	27	°C
Evaporator air mass flow rate	0.3	kg/s
Internal HX effectiveness	0.6	-
Internal HX suction inlet quality	0.95	-
Gas cooler refrigerant outlet temperature	$T_{amb} + 5$	°C

4.1 Effect of high-side pressure

In transcritical CO_2 systems, unlike subcritical refrigeration cycles, the high-side pressure is independent of the gas cooler exit temperature. The system COP can be improved by changing the high-side pressure. Figure 5(a) shows change in COP and Figure 5(b) shows the increase in cooling capacity for four combinations involving Evap A only as high-side pressure is changed. The simulations are run at a compressor speed of 1200min⁻¹, ambient temperature of 35°C, while keeping the evaporator exit conditions at a superheat of 5°C. The COP reaches peak at a certain value of high-side pressure. Combinations having Comp A (Comb 1 & 3) performs better than the combinations having Comp B (Comb 5 & 7). Similarly, the combinations having Ejec B (Comb 3 & 7) performs better than the combinations having Ejec A. The maximum COP is for Comb 3 having Comp A and Ejec B. The system capacity is also highest for the Comb 3. The performance difference between Comb 1 and Comb 5 is consistent with the experimental data.

| (a) | (b) |
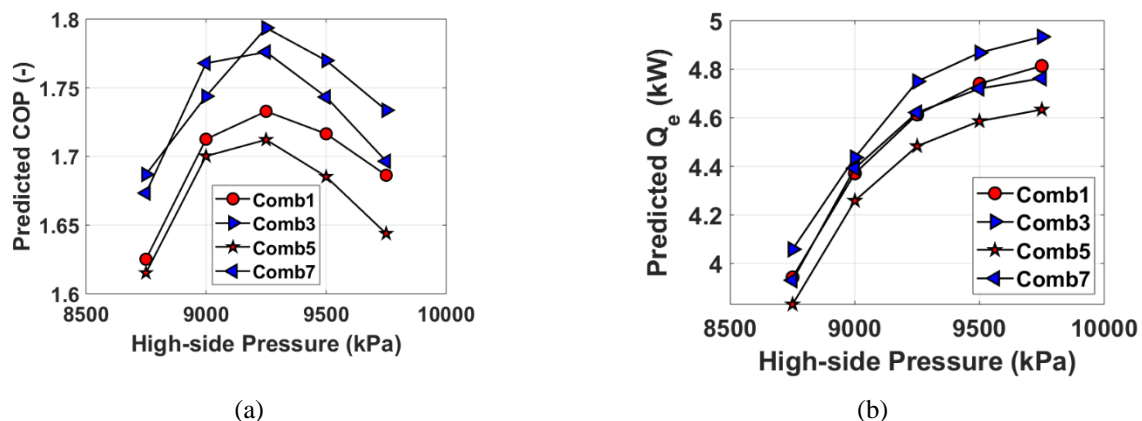
Figure 5: High-side pressure effect on system performance (a) COP (b) Q_e for selected system combinations

In following subsections, the system performance is evaluated at different high-side pressures. However, only the maximum COP and corresponding cooling capacity is reported.

4.2 Effect of compressor speed

The system model is evaluated for predicting performance of four combinations having Evap B only at different compressor speeds. The evaporator exit conditions are at a superheat level of 5°C and system is run at an ambient temperature of 35°C. Figure 6(a) shows that the Comb 4 has the highest COP at any given compressor speed as compared to other combinations. The Comb 2 and Comb 4 having Comp A has similar trends, whereas the performance trends for Comb 6 and Comb 8 having Comp B are similar. The systems with Comp A have better performance than the systems with Comp B in general. Ejec B improves the performance of the system greater than Ejec A. The effect of Ejec B is significant in Comb 8 for compressor speed 1100-1300 as Comb 8 works better than Comb 2. The cooling capacities for the system with Comp B (Comb 2 and Comb 4) in Figure 6(b) remain greater than the systems with Comp A (Comb 6 and Comb 8).
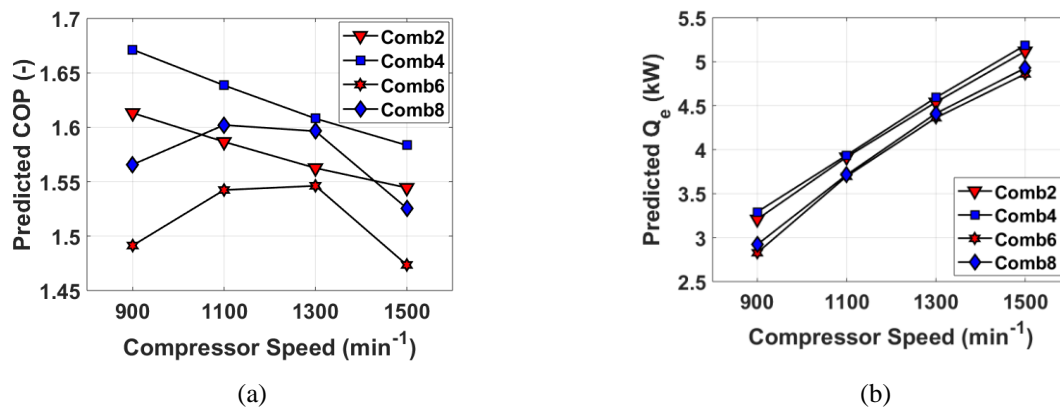
Figure 6: Effect of changing compressor speed on performance (a) COP (b) Q_e for selected system combinations

4.3 Effect of evaporator exit conditions

The system model is simulated for four combinations involving Comp A only. The evaporator exit conditions are changed from single-phase to two-phase flow conditions. The system is simulated at an ambient temperature of 35°C, and for a compressor speed of 1200min^{-1}. Figure 7(a) shows that the system COP is maximum when evaporator exit conditions are saturated vapor for all the combinations. The combinations with Ejec B perform better. Also, the combinations using Evap A performs better than Evap B with only one exception, i.e., Comb 1 performs better than Comb 4 for superheated exit conditions.
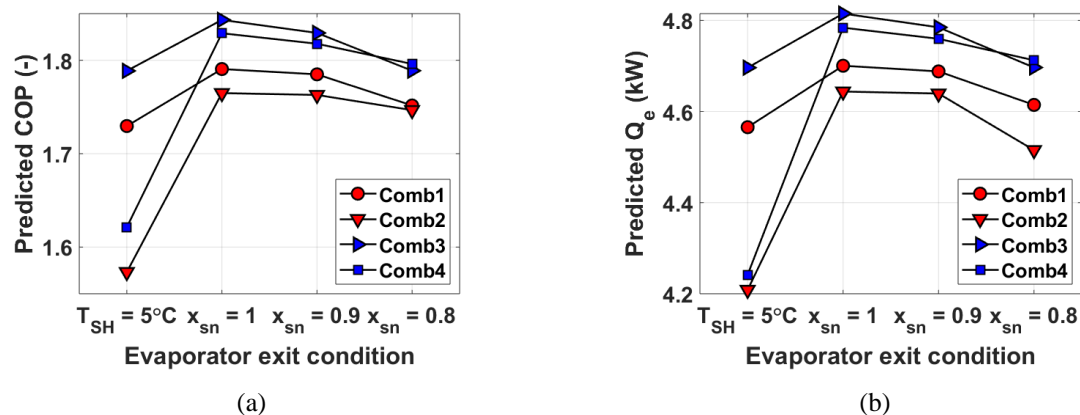
Figure 7: Effect of changing evaporator exit conditions on (a) COP (b) Q_e for selected system combinations

4.4 Effect of ambient conditions

The transcritical CO_2 system performance decreases when it is operated at higher ambient temperatures. All the combinations of Comp A are simulated for four different ambient temperatures. The compressor speed is kept at 1200min^{-1}, while evaporator exit is set to have a saturated vapor condition. Figure 8(a) shows that the COP drops around 60%, whereas Figure 8(b) shows that the capacity drops around 20% for each of the combination as ambient temperature is changed from 35°C to 50°C. The performance of systems having Ejec B remains better than the system

with Ejec A. The Comb 3 and Comb 4 have almost the same performance for saturated vapor evaporator exit conditions.

(a)   (b)
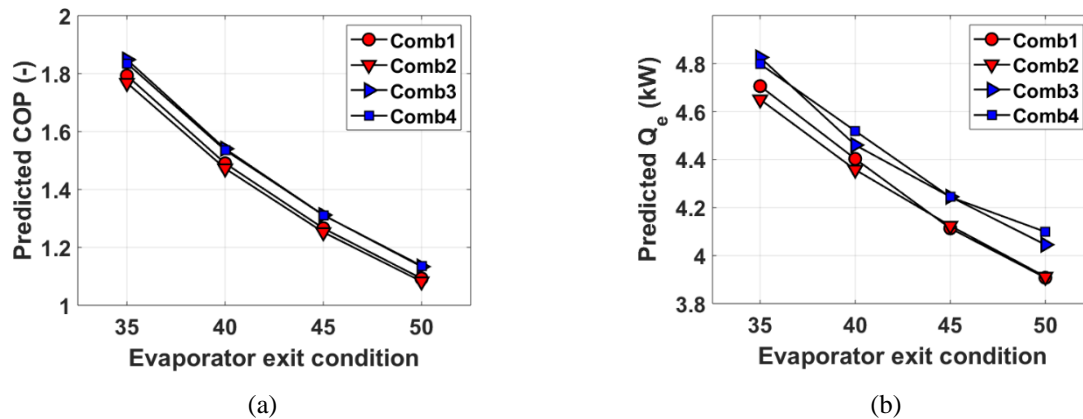
Figure 8: Effect of ambient temperature on performance (a) COP (b) Q_e for selected system combinations

4.5 Comparing the best and the worst component combination

From above analysis, Comb 3 having Comp A, Ejec B, and Evap A is giving best performance, whereas Comb 6 having Comp B, Ejec A, and Evap B has the lowest performance. The performance of the two systems is compared at a compressor speed of 1200min^{-1}, ambient temperature of 35°C, and an evaporator exit of saturated vapor. These conditions are expected to give the maximum performance for Comb 6. The analysis shows that the system COP and cooling capacity of Comb 3 is 5.3% and 6.4% higher, respectively, than that of Comb 6. Figure 9(a) and Figure 9(b) shows Ph and Ts-diagram for Comb 3 and Comb 6, respectively. The evaporator temperature in Comb 3 is relatively lower than it is in Comb 6, which can explain for higher cooling capacity. However, the higher pressure rise due to Ejec B in Comb 3 makes the compressor suction inlet conditions similar in both systems, resulting in higher COP.

(a)   (b)
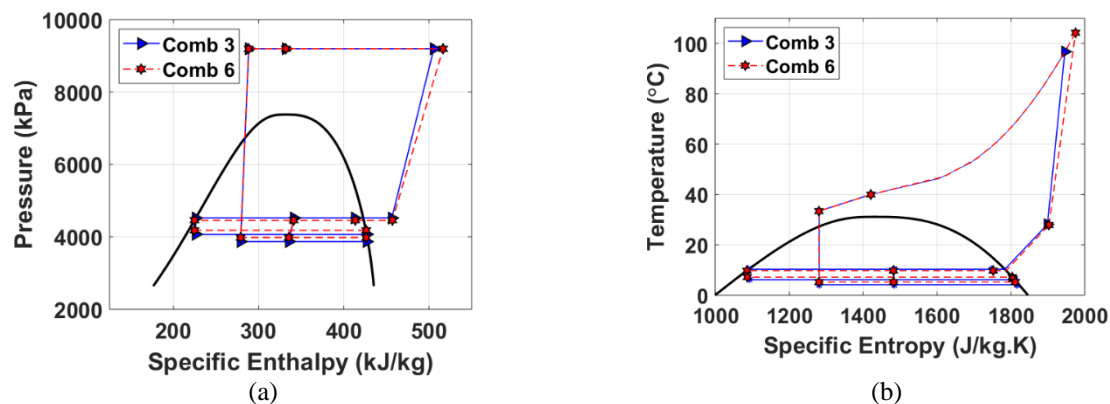
Figure 9: Comparison of (a) Ph and (b) Ts-diagram for Comb 3 (best) with Comb 6 (worst) system combinations

The best system combination has been identified as Comb 3. The ejector performance maps have been crucial in predicting wide range of operating conditions in making this decision. However, the evaporator model is found to be the most computationally expensive component model.

5. CONCLUSIONS

In this paper, a systematic study is undertaken for designing a transcritical CO_2 ejector air conditioning system using the advantage of newly proposed ejector performance maps. A system model is developed from component models that have been validated against the experimental data. An enthalpy marching algorithm is used in solving the system.

A total of eight combinations have been investigated while studying the effects of high-side pressure, compressor speed, evaporator exit conditions, and ambient temperature. It is found that the Comb 3 using Comp A, Ejec B and

Evap A gives the best performance for wide range of operating conditions. The study has found that an improvement of 5.3% in COP and 6.4% in cooling capacity is possible simultaneously while comparing the best and the worst performing component combinations.

The results are very promising in making ejector system selection decision an easier task. However, computationally efficient evaporator models along with modeling of IHX and gas cooler need to be undertaken to expand the scope of system analysis. The ejector performance maps should be utilized in system designing of other refrigerant systems as well.

NOMENCLATURE

C	swept volume of compressor	(m^3)
Comp	referring to either Comp A or Comp B	(-)
Ejec	referring to either Ejec A or Ejec B	(-)
Evap	referring to either Evap A or Evap B	(-)
h	specific enthalpy	(kJ/kg)
IHX	Internal Heat Exchanger	(-)
$\dot{m}$	mass flow rate	(kg/s)
N	compressor speed	(min^{-1})
P	pressure	(kPa)
s	specific entropy	(kJ/kgK)
T	temperature	(°C)
$\dot{W}$	power	(W)
x	quality	(-)
$\hat{X}$	predicted compressor efficiencies	(-)
β	pressure ratio	(-)
ϕ_m	mass entrainment ratio	(-)
ϕ_v	volumetric entrainment ratio	(-)
$\eta_{ejec,map}$	ejector efficiency	(-)
ρ	density	(kg/m^3)
$\hat{\eta}$	predicted efficiency	(-)

Subscript	
act	referring to actual work
amb	ambient
cpri	compressor refrigerant inlet
elec	referring to electric work
eri	evaporator refrigerant inlet
isen	referring to isentropic work
meas	measured
mn	motive nozzle
norm	normalized
SH	super heat
sn	suction nozzle
suc	compressor suction

REFERENCES

Aidoun, Z., Ameur, K., Falsafioon, M., Badache, M., 2019. Current Advances in Ejector Modeling, Experimentation and Applications for Refrigeration and Heat Pumps. Part 2: Two-Phase Ejectors. Inventions, 4(1), 16.

Banasiak, K., Hafner, A., Kriezi, E.E., Madsen, K.B., Birkelund, M., Fredslund, K., Olsson, R., 2015, Development and performance mapping of a multi-ejector expansion work recovery pack for R744 vapour compression units, Int. J. Refrigeration, 57: 265-276.

Bell, I. H.; Wronski, J.; Quoilin, S.; Lemort, V. Pure and pseudo-pure fluid thermophysical property evaluation and the open-source thermophysical property library Coolprop. Ind. Eng. Chem. Res. 2014, 53, 2498−2508

Churchill, S.W., 1977, Friction factor equations spans all fluid-flow regimes, Chem. Engr., 84(24): 91-92.

Elbel, S., Hrnjak, P., 2008, Experimental validation of a prototype ejector designed to reduce throttling losses encountered in transcritical R744 system operation, Int. J. Refrigeration, 31: 411-422.

Friedel, L., 1979, Improved friction pressure drop correlations for horizontal and vertical two-phase pipe flow, European Two Phase Flow Group Meeting, Ispra, Italy, Paper E2.

Gnielinski, V., 1976, New equations for heat and mass transfer in turbulent pipe and channel flow, Int. Chem. Engr., 16(2): 359-367.

Haider, M., Elbel, S., 2020. Development of a new ejector performance map for design of an automotive air conditioning system. SAE World Congress, Detroit, MI, USA, April 21-23, Paper 2020-01-1244.

Lawrence, N., Elbel, S., "Numerical investigation of the effect of microchannel evaporator design and operation on the improvement potential of ejector refrigeration cycles," Energy, pp. 21-34, 2018.

Nakagawa, M., Marasigan, A. R., Matsukawa, T., 2011, Experimental analysis on the effect of internal heat exchanger in transcritical CO2 refrigeration cycle with two-phase ejector Int J. Refrigeration 34, 1577-1586.

Palacz, M., Smolka, J., Kus, W., Fic, A., Bulinski, Z., Nowak, A. J., Banasiak K., Hafner, A., 2016, CFD-based shape optimisation of a CO2 two-phase ejector mixing section, Appl. Thermal Engineering, pp. 62-69.

Park, Y., Jacobi, A.M., 2009, Air-side heat transfer and friction correlations for flat-tube louver-fin heat exchangers, ASME J. Heat Transfer, 131, 021801.

Pottker, G., Hrnjak, P., 2015, Ejector in R410A vapor-compression systems with experimental quantification of two major mechanisms of performance improvement: Work recovery and liquid feeding, Int. J. Refrigeration, 50: 184-192.

Shah, M. M., 2017, Unified correlation for heat transfer during boiling in plain mini/micro and conventional channels, Int. J. Refrigeration, 74: 606-626.

Smołka, J., Buliński, Z., Fic, A., Nowak, A.J., Banasiak, K., Hafner, A., 2013, A computational model of a transcritical R744 ejector based on a homogeneous real fluid approach, Appl. Math. Modeling, 37: 1208-1224.

Winkler, J., Aute, V., Radermacher, R., 2008, Comprehensive investigation of numerical methods in simulating a steady-state vapor compression system, International Journal of Refrigeration 31 (2008) 930-942.

Zhu, J., Botticella, F., Elbel, S., 2018, "Experimental investigation and theoretical analysis of oil circulation rates in ejector cooling cycles," Energy, pp. 718-733.

Zhu, Y., Li, C., Zhang, F., Jiang, P.-X., 2017. Comprehensive experimental study on a transcritical CO2 ejector-expansion refrigeration system. Energy Conversion and Management. 151, 98-106.

ACKNOWLEDGEMENT